









Nitrogen nutrition effects on $\delta^{13}\text{C}$ of plant respired CO_2 are mostly caused by concurrent changes in organic acid utilisation and remobilisation

Yang Xia^{1,2}  | Julie Lalande³ | Franz-W. Badeck⁴  | Cyril Girardin⁵  | Camille Bathellier⁶  | Gerd Gleixner⁷  | Roland A. Werner⁸  | Shiva Ghiasi^{8,9} | Mélodie Faucon¹ | Karen Cosnier¹ | Chantal Fresneau¹ | Guillaume Tcherkez^{3,10}  | Jaleh Ghashghaie¹ 

¹Université Paris-Saclay, CNRS, AgroParisTech, Ecologie Systématique et Evolution (ESE), Gif-sur-Yvette, France

²College of Life Science and Oceanography, Shenzhen University, Shenzhen, China

³Institut de recherche en horticulture et semences, UMR 1345, Université d'Angers, SFR Quasav, Beaucozé, France

⁴Research centre for Genomics & Bioinformatics (CREA- GB), Council for Agricultural Research and Economics, Fiorenzuola d'Arda, Italy

⁵Université Paris-Saclay, INRAE, UMR 1402 ECOSYS, Campus Agro Paris-Saclay, Palaiseau, France

⁶Centre d'affaires ATEAC, Elementar France, Lyon, France

⁷Max Planck Institute for Biogeochemistry, Jena, Germany

⁸Institute of Agricultural Sciences, ETH Zurich, Zurich, Switzerland

⁹Department Agroecology and Environment, Agroscope, Zurich, Switzerland

¹⁰Research school of biology, Australian National University, Canberra, Australian Capital Territory, Australia

Correspondence

Jaleh Ghashghaie, Université Paris-Saclay, CNRS, AgroParisTech, Ecologie Systématique et Evolution (ESE), 91190, Gif-sur-Yvette, France.

Email: jaleh.ghashghaie@universite-paris-saclay.fr

Funding information

Région Pays de la Loire and Angers Loire Métropole; China Scholarship Council

Abstract

Nitrogen (N) nutrition impacts on primary carbon metabolism and can lead to changes in $\delta^{13}\text{C}$ of respired CO_2 . However, uncertainty remains as to whether (1) the effect of N nutrition is observed in all species, (2) N source also impacts on respired CO_2 in roots and (3) a metabolic model can be constructed to predict $\delta^{13}\text{C}$ of respired CO_2 under different N sources. Here, we carried out isotopic measurements of respired CO_2 and various metabolites using two species (spinach, French bean) grown under different $\text{NH}_4^+:\text{NO}_3^-$ ratios. Both species showed a similar pattern, with a progressive ^{13}C -depletion in leaf-respired CO_2 as the ammonium proportion increased, while $\delta^{13}\text{C}$ in root-respired CO_2 showed little change. Supervised multivariate analysis showed that $\delta^{13}\text{C}$ of respired CO_2 was mostly determined by organic acid (malate, citrate) metabolism, in both leaves and roots. We then took advantage of nonstationary, two-pool modelling that explained 73% of variance in $\delta^{13}\text{C}$ in respired CO_2 . It demonstrates the critical role of the balance between the utilisation of respiratory intermediates and the remobilisation

This is an open access article under the terms of the [Creative Commons Attribution-NonCommercial-NoDerivs](https://creativecommons.org/licenses/by-nc-nd/4.0/) License, which permits use and distribution in any medium, provided the original work is properly cited, the use is non-commercial and no modifications or adaptations are made.

© 2024 The Author(s). *Plant, Cell & Environment* published by John Wiley & Sons Ltd.

of stored organic acids, regardless of anaplerotic bicarbonate fixation by phosphoenolpyruvate carboxylase and the organ considered.

KEYWORDS

ammonium:nitrate ratio, anaplerosis, carbon isotope fractionation, respiration

1 | INTRODUCTION

C₃ plant photosynthesis discriminates between CO₂ isotopologues so that photosynthates are naturally ¹³C-depleted compared to atmospheric carbon dioxide. Furthermore, the carbon isotope composition (δ¹³C) in plant organic matter is also the result of CO₂ loss by respiration, which may be associated with ¹²C/¹³C isotope fractionations. In the past two decades, plant respiration has received increasing attention because of its possible influence on plant and ecosystem ¹³C budgets. There is now compelling evidence that leaf dark respiration usually generates ¹³C-enriched CO₂ (up to 10% compared to total organic matter) while often root respiration produces relatively ¹³C-depleted CO₂ (Ghashghaie & Badeck, 2014). Using plants grown under controlled mesocosm conditions, it has been suggested that at the plant scale, the ¹³C-enrichment caused by leaf respiratory carbon loss is compensated for by the ¹³C-depletion caused by root respiration, thus with little overall effect of respiration (Bathellier et al., 2008; Klumpp et al., 2005).

However, δ¹³C of leaf-respired CO₂ varies considerably between species and depends on environmental conditions (e.g. drought, temperature), the availability of respiratory substrates (carbohydrates, lipids or proteins) and the relative activity of metabolic pathways (Bathellier et al., 2017). In the short- or midterm, this has important consequences for δ¹³C of CO₂ in air in terrestrial ecosystems. For example, it has been shown that during the night, the impact of changes in leaf respiratory metabolism influences ecosystem-respired CO₂, in a temperature-dependent manner (Knohl et al., 2005; Werner & Gessler, 2011; Werner et al., 2007). Leaf respiration can also have an enormous impact on measured photosynthetic isotope discrimination (Δ_{obs}) in particular when respiration uses substrates disconnected from photosynthates (i.e. non-photosynthetic carbon source) and net CO₂ assimilation is low (Barbour et al., 2017). In crops like wheat, the respiratory loss has an impact on δ¹³C of grains, in proportion with carbon use efficiency (i.e. percentage of carbon lost by respiration) and harvest index (Domergue, Abadie, et al., 2022). Taken as a whole, the isotope composition of respired CO₂ is of crucial importance for understanding plant and ecosystem carbon balance. However, there is presently no clear empirical relationship or equation predicting δ¹³C of respired CO₂, and this represents a hurdle in plant ¹³C budget modelling.

In principle, δ¹³C of respired CO₂ should depend on both metabolic pathways (i.e. δ¹³C of source carbon and metabolic fluxes) and isotope effects associated with enzymes involved therein. Using biochemical degradation or ¹³C-NMR, it has been shown that within

the glucose molecule, δ¹³C of C-atom positions differ, with C-3 and C-4 positions being relatively ¹³C-enriched (Gilbert et al., 2012; Rossmann et al., 1991). As a result, pyruvate molecules produced by glycolysis are probably ¹³C-enriched in C-1 (COOH group) and ¹³C-depleted in C-2 (C = O) and C-3 (CH₃) atom positions. Consequently, CO₂ liberated from position C-1 by pyruvate dehydrogenase should be ¹³C-enriched. This intramolecular effect is believed to be the at the origin of the ¹³C-enrichment in leaf-respired CO₂ (Bathellier et al., 2017; Ghashghaie & Badeck, 2014; Tcherkez et al., 2003). The relative ¹³C-depletion in glucose (in positions other than C-3 and C-4) probably also leads to a ¹³C-depletion in CO₂ produced by the oxidative pentose phosphate pathway (OPPP) which comes from glucose C-1 atom position. Experiments using positionally ¹³C-labeled substrates (i.e. glucose and pyruvate) have shown a substantial OPPP activity in roots (22% of CO₂ production rate) and thus, the OPPP likely contributes to explaining the natural ¹³C-depletion in root-respired CO₂ (Bathellier et al., 2009). The utilisation of substrates other than glucose by catabolism influences δ¹³C of respired CO₂. For example, lipids are naturally ¹³C-depleted and their degradation leads to a ¹³C-depletion in leaf-respired CO₂ during prolonged darkness (Tcherkez et al., 2003). Organic acids coming from anaplerotic, phosphoenolpyruvate carboxylase (PEPC)-catalysed fixation are ¹³C-enriched and thus their decarboxylation generates ¹³C-enriched CO₂. This phenomenon has been shown to occur during light-enhanced dark respiration in leaves (respiratory peak after illumination) (Barbour et al., 2007; Gessler et al., 2009; Lehmann et al., 2016; Priault et al., 2009).

Respired CO₂ is the net result of several (de)carboxylation reactions (pyruvate dehydrogenase, Krebs cycle decarboxylation, OPPP, PEPC) and thus it depends on the respective contribution of such reactions. This in turn depends on physiological conditions, since the utilisation of carbon skeletons generated by catabolism varies with the physiological status of the plant, environmental cues, nutrients and species. In particular, nitrogen nutrition has a strong effect on respiratory metabolism, since N assimilation abstracts 2-oxoacids (such as 2-oxoglutarate) to form amino acids (such as glutamate). For example, it is well known that nitrate utilisation is associated with an increase in glycolysis, anaplerotic fixation and a decrease in sugar concentration in leaves (Krapp et al., 2014; Stitt et al., 2002). Therefore, N availability should impact on δ¹³C of respired CO₂. In fact, we have previously shown in tobacco (*Nicotiana tabacum*) that the balance between ammonium and nitrate has an influence on δ¹³C of leaf-respired CO₂, with a progressive ¹³C-depletion as the proportion of ammonium as a N source increased (Ghiasi et al., 2021). In addition, we suggested that this

was partly explained by the contribution of organic acid metabolism. In effect, there was a strong relationship between $\delta^{13}\text{C}$ of CO_2 and that in organic acids (malate, citrate). Since the ^{13}C -enrichment in organic acids likely comes from PEPC activity which fixes naturally ^{13}C -enriched HCO_3^- (for a review of isotope effects in enzymes, see Tcherkez et al., 2011), $\delta^{13}\text{C}$ variations in respired CO_2 can be viewed as reflecting changes in the metabolic flux associated with PEPC activity. However, nitrate assimilation does not only involve leaves since some proportion of absorbed nitrate is reduced in roots (up to 30%, depending on species) (Andrews, 1986). In addition, when nitrate is balanced against ammonium, a specific effect of ammonium metabolism could be expected. NH_4^+ is rapidly consumed by the glutamine synthetase/glutamine 2-oxoglutarate aminotransferase (GS-GOGAT) pathway, causes an increase in root respiration rate leading to the biosynthesis of N-rich compounds such as amides, polyamines and/or ureides (González-Moro et al., 2021; Xiao et al., 2023). Therefore, consequences of N nutrition on $\delta^{13}\text{C}$ of root-respired CO_2 can be anticipated.

Here, we looked at changes in $\delta^{13}\text{C}$ of respired CO_2 in both leaves and roots in spinach (*Spinacia oleracea*) and French bean (*Phaseolus vulgaris*) plants grown with varying proportions of NH_4^+ and NO_3^- fertilizers in the nutrient solution. These two species were selected due to their agronomic importance and their contrasting behaviour with respect to nitrogen use (spinach is nitrophilous, while bean naturally involves ureide metabolism and can have N_2 -fixing nodules). We first used N isotopes to check whether plants used ammonium and nitrate according to the proportion imposed with the nutrient solution. We then took advantage of compound-specific isotope analyses to compare $\delta^{13}\text{C}$ of CO_2 with that of metabolites (such as sugars and organic acids) and determined the respiration rate and PEPC activity. We integrated the data using multivariate statistics and nonstationary mechanistic modelling to elucidate best candidate drivers and design a predictive model of $\delta^{13}\text{C}$ in respired CO_2 . Our working questions were: (1) is there a consistent $\delta^{13}\text{C}$ pattern in respired CO_2 as the ammonium-to-nitrate ratio varies, in leaves and roots? (2) which metabolites influence most $\delta^{13}\text{C}$ of respired CO_2 ? (3) is it possible to construct a metabolic model of $\delta^{13}\text{C}$ of respired CO_2 that can be applied regardless of N conditions, species, and organs?

2 | MATERIAL AND METHODS

2.1 | Plant material

French bean (*Phaseolus vulgaris* L.) cv. *Contender*, and spinach (*Spinacia oleracea* L.) cv. *Géant d'Hiver* were purchased from Vilmorin (France). Seeds were germinated in vermiculite with tap water in darkness. Seven days old seedlings were transplanted to pots (8.3 cm diameter, 11 cm height; one plant per pot) filled with sand (previously washed with tap water and sterilised in an autoclave) and grown in the greenhouse. Whole culture duration was 33 and 38 d for bean and spinach, respectively. Under our conditions (sufficient total N

availability), bean plants did not form nodules. Bean plants were grown in January 2017 under natural light, with supplementary light supplied by lamps (Metal Halide Lamps, HSI-THX, 400 W, Sylvania) 10 h per day, providing a photosynthetic photon flux density (PPFD) of 140–160 $\mu\text{mol photons m}^{-2} \text{s}^{-1}$ at plant height. Air temperature was $23 \pm 2^\circ\text{C}$ during the day and $17 \pm 2^\circ\text{C}$ at night. Humidity was $42\% \pm 8\%$ during the day and $55\% \pm 15\%$ at night. Spinach plants were grown in July and August 2017, with an artificial light source (200–210 $\mu\text{mol photons m}^{-2} \text{s}^{-1}$ PPFD at plant height) only 16 h per day. Temperature and humidity were the same as for bean cultivation. Maize plants were grown at the same time to have an indirect measurement of ambient CO_2 using maize leaf organic matter. The carbon isotope composition of the ambient CO_2 in the culture rooms was about -9.5% (measured, Vienna-Pee Dee Belemnite as standard) and -14.1% (estimated, considering $\delta^{13}\text{C}$ of maize) for bean and spinach, respectively. In figures below, the difference between maize leaf and bean or spinach organic matter (weighted average of root and leaf $\delta^{13}\text{C}$) is referred to as $^{\text{Maize}}\Delta\delta_{\text{TOM}}$.

2.2 | Nutrient conditions

Plants were supplied with nutrient solutions with 6 different proportions of ammonium (NH_4^+) and nitrate (NO_3^-) as N source as follows ($\text{NH}_4^+/\text{NO}_3^-$ ratios): 0/100, 25/75, 50/50, 75/25, 90/10 and 100/0. In the following, N-treatments are referred to proportions of NH_4^+ (i.e. 0%, 25%, 50%, 75%, 90% and 100%, respectively). Nutrient solutions contained 6 mmol L^{-1} of N (total) formed with a combination of KNO_3 , $\text{Ca}(\text{NO}_3)_2$, NH_4NO_3 or $(\text{NH}_4)_2\text{SO}_4$ to obtain different N-treatments. Additional components were: 1 mM CaCl_2 , 0.25 mM KH_2PO_4 , 1 mM MgSO_4 , and trace elements (2 μM MnSO_4 , 2 μM ZnSO_4 , 0.5 μM CuSO_4 , 25 μM $\text{B}(\text{OH})_3$, 0.5 μM Na_2MoO_4 , 40 μM Fe-EDTA). The pH of solutions was kept constant at 5.5. In 100% NH_4^+ and 90% NH_4^+ treatments, 1 mM K_2SO_4 was added to keep K concentration constant. Although the sand was sterilised by autoclaving, 1 ppm nitrification inhibitor (2-chloro-6-trichloromethylpyridine) was added to nutrient solutions for spinach, to avoid contamination by nitrifying bacteria from the environment. Nutrient solutions were used for watering the plants only after appearance of cotyledons (750 mL solution plate $^{-1}$ d $^{-1}$, with 8 pots in each plate). The amount of the solution was so that pots reached full capacity and allowed to drain to plates. During the last week before harvesting, the amount of the solution was increased to 1000–1500 mL plate $^{-1}$ d $^{-1}$ depending on plant growth rate. Chlorophyll content and Nitrogen Balance Index were measured every 3 days with a DUALEX instrument (DUALEX SCIENTIFIC + TM, ForceA, France, Orsay) to check plants were not N deficient.

2.3 | Leaf gas exchange parameters

One month after planting, gas exchange and chlorophyll fluorescence were measured using a Licor 6400 with LCF chamber (LI-COR, Inc.) in

the morning (9–12 h) during 3 successive days. One plant with mature leaves was selected from each treatment each day. Therefore, there were 3 replications for gas exchange measurement. Plants used for measurement were selected randomly. Before photosynthetic measurements, plants were dark-adapted for 30 min, then one mature leaf was used. Gas exchange conditions were set as follows: flow rate $300 \mu\text{mol air s}^{-1}$, CO_2 mole fraction $390 \mu\text{mol mol}^{-1}$ and PPFD $400 \mu\text{mol m}^{-2} \text{s}^{-1}$ (with 10% blue). Leaf temperature was fixed at 22°C . Leaf net CO_2 assimilation rate (A_n), stomatal conductance (g_s) and the ratio of intercellular to ambient CO_2 concentrations (C_i/C_a) data were automatically recorded every 3 min, reaching steady values after about 30 min. Three values in the steady state were recorded to get a mean value for each plant.

2.4 | Carbon isotope composition of respired CO_2

To ensure that plants had enough photosynthates as (potential) respiratory substrates, they were taken from the greenhouse after at least 4 h light. They were then placed in the dark for 30 min to avoid light enhanced dark respiration (LEDR). One intact mature leaf was cut off and put into a flask (50 mL) completely covered by aluminium foil. The flask was flushed with CO_2 -free air for 5 min, then sealed with a septum and left for respired CO_2 accumulation. CO_2 concentration was analysed by micro-GC (490 Micro GC, Agilent Technologies), with an injection volume of $5 \mu\text{L}$ every 3 min. When CO_2 mole fraction was above $1000 \mu\text{mol mol}^{-1}$ (approximately after 12 min), air samples were manually collected from the flask with a syringe (0.5 to 1 mL depending on CO_2 concentration) and injected into a GC-IRMS, made of a gas chromatograph (GC HP 5890) coupled to a stable isotope ratio mass spectrometer (Optima Isochrom- μG , Fisons Instruments) to measure the carbon isotope composition of respired CO_2 (denoted as $\delta^{13}\text{C}_R$). Syringes were flushed with helium five times and then with sample air inside a given flask 10 times before each injection. Each flask was sampled and measured 3 times to ensure reproducibility of measurements. For root-respired CO_2 , roots were first washed with tap water and dried with absorbing paper before incubation in flasks. Since the respiration rate and the size of roots were greater than that of leaves, bigger flasks (120 mL) were used. Measurements were made between 10:00 and 16:00 each day, and with a random selection of plants.

2.5 | Sampling

Plants used for measurements of $\delta^{13}\text{C}$ in respired CO_2 were harvested for biomass determination. Plants were divided into leaves, stems and roots. Samples were plunged into liquid nitrogen and then freeze-dried. Samples were then ground into a fine powder (using a Retsch MM200 mill ball, Bioblock Scientific) used for isotope measurements and extractions.

2.6 | Extraction of soluble fraction

Plant powder (50 mg) was suspended in 1 mL cold distilled water and maintained on ice for 60 min with agitation with vortex every 10 min. After centrifugation ($14,000 \text{ g}$, 5°C , 15 min), the supernatant (containing soluble sugars, organic and amino acids and soluble proteins) was separated from the pellet. The supernatant was heated at 100°C for 5 min and then kept on ice for 30 min to precipitate heat-denatured proteins. After centrifugation ($14,000 \text{ g}$, 5°C , 15 min), the soluble fraction was collected, kept at -20°C for subsequent utilisation. Samples were referred to as water soluble organic matter (WSOM). Aliquots of $200 \mu\text{L}$ were poured into tin capsules and oven-dried at 50°C for isotope analysis.

2.7 | Carbon and nitrogen isotope composition of organic material

Carbon and nitrogen isotope composition of bulk organic matter ($\delta^{13}\text{C}_{\text{OM}}$ and $\delta^{15}\text{N}_{\text{OM}}$) was determined using powdered dry material. $600\text{--}800 \mu\text{g}$ were weighed in tin capsules (Courtage Analyse Service). $\delta^{13}\text{C}$ was measured with an elemental analyser (Flash EA) coupled to a Delta Plus XP isotope ratio mass spectrometer via a 6-port valve and a ConFlo III interface (Finnigan MAT). The positioning of samples, blanks, laboratory standards and quality control standards in a measurement sequence followed the scheme described previously (Werner et al., 1999). The carbon and nitrogen isotope composition ($\delta^{13}\text{C}$, $\delta^{15}\text{N}$) were calculated as relative difference in the isotope ratio (R) from the international standard (Vienna-Pee Dee Belemnite, air, respectively):

$$\delta(\text{‰}) = [(R_{\text{sample}} - R_{\text{standard}}) / R_{\text{standard}}] \cdot 1000$$

2.8 | Compound-specific isotope analysis

The $\delta^{13}\text{C}$ of common organic acids (malate and citrate) and main sugars (sucrose, glucose and fructose) were determined using liquid chromatography coupled to isotope ratio mass spectrometry (IRMS) as in (Ghiasi et al., 2021). Briefly, WSOM extracts were diluted 500 times, and the pH was adjusted to 7. Then 4 mL were passed through cation exchangers (DionexTM OnGuard II H 1.0 cc cartridges, Thermo Scientific) and anion exchangers (DionexTM OnGuard II A 1.0 cc cartridges) to retain amino acids and organic acids, respectively, and collect soluble sugars. Purified soluble sugars were collected in amber silanised glass vials (Vial short tread, VWR International). Organic acids were collected in amber glass vials. The Thermo Finnigan LC-IsoLink system (Ultimate 3000, Dionex/Thermo Scientific) coupled to Delta V Advantage isotope ratio mass spectrometer (Thermo Scientific) was used for $\delta^{13}\text{C}$ of individual soluble sugars and organic acids (malate and citrate). Amounts (denoted as [C]) and $\delta^{13}\text{C}$ of individual sugars were used to calculate $\delta^{13}\text{C}$ of total soluble sugars ($\delta^{13}\text{C}_{\text{Sug}}$) using mass balance, as $\delta^{13}\text{C}_{\text{Sug}}(\text{‰}) = (\delta^{13}\text{C}_{\text{Glc}} \cdot [\text{C}]_{\text{Glc}} + \delta^{13}\text{C}_{\text{Suc}} \cdot [\text{C}]_{\text{Suc}} + \delta^{13}\text{C}_{\text{Fru}} \cdot [\text{C}]_{\text{Fru}}) / ([\text{C}]_{\text{Glc}} + [\text{C}]_{\text{Suc}} + [\text{C}]_{\text{Fru}})$. Similarly, using

amounts and $\delta^{13}\text{C}$ of individual sugars and organic acids, we calculated the predicted $\delta^{13}\text{C}$ of total water-soluble fraction to compare with measured values ($\delta^{13}\text{C}_{\text{WSOM}}$).

The $\delta^{13}\text{C}$ of the most abundant free fatty acid (palmitic or palmitic acid depending on species; simply referred to as "palmitate" thereafter), maltose and amino acids was determined on derivatised samples (methoxyamine and MSTFA in pyridine) using gas chromatography coupled to IRMS using a GC 7693A coupled to a combustion module GC5 (filled with the GCN reactor) and precISION IRMS (Elementar), after (Domergue, Lalande, et al., 2022). Isotope standards were caffeine (IAEA-600) and nicotine (home standard, from Sigma-Aldrich/Merck) and retention time indices were obtained using an alkane mix (injected separately; Connecticut n-Hydrocarbon Mix, Supelco). Specific standards of known $\delta^{13}\text{C}$ were used to determine the $\delta^{13}\text{C}$ of trimethylsilyl (TMS) groups (-33.32‰) and thus correct the $\delta^{13}\text{C}$ of analytes (palmitate 1 TMS, maltose 8 TMS, and TMS derivatives of amino acids) for the contribution of TMS carbons to raw isotope composition. $\delta^{13}\text{C}$ was corrected for linearity to account for the fact that some metabolites were more abundant than others (in practice this correction was small, generally less than 0.2‰). The weighted-average $\delta^{13}\text{C}$ of amino acids was calculated using the observed signal (mass-44) and $\delta^{13}\text{C}$ of individual amino acids.

2.9 | PEPC activity

Samples used for PEPC activity were periodically harvested during the daytime and conserved at -80°C. 150 mg frozen roots or leaves (without petioles and midribs) were ground in a mortar with liquid nitrogen with 100 mg sand. Then 1 mL extraction buffer (HEPES 50 mM; MgCl₂ 10 mM; EDTA 1 mM; EGTA 1 mM; BSA 0.025% (w/v); glycerol 10% (w/v); DTT 5 mM and protease inhibitor) was added (4°C). After agitation with a vortex for 2 s, the sample was thawed on ice and agitated again with a vortex for 5 s and centrifuged at 10,000 g, 4°C for 10 min. PEPC activity was measured using a coupled reaction assay (NADH-oxidation via malate dehydrogenase). The assay medium contained 2 mM phosphoenolpyruvate (PEP), 100 mM Tricine (pH 8.0), 10 mM NaHCO₃, 20 mM MgCl₂, 0.05% Triton, 0.5 mM NADH, 1 U mL⁻¹ malate dehydrogenase, 20 µL enzyme extraction solution, with 200 µL as the final volume. Two technical replicates for each sample were measured. Measurements used a 96-well plate placed in a microplate spectrophotometer (PowerWave HT, BioTek) to record NADH oxidation at 340 nm averaged across 20 min. A blank without PEP was also recorded for subtraction. An assay where PEP was replaced by H₂O was checked as a control. PEPC activity was calculated as the blank-corrected difference in NADH oxidation rate before and after the addition of PEP.

2.10 | Statistics

Omics analyses were carried out on 3 to 4 samples per condition and species (i.e., 4 independent replicate). Univariate statistical analysis

was conducted using an analysis of variance (one-way ANOVA) to examine differences between NH₄⁺:NO₃⁻ conditions (Figures 1–4). The data were also analysed via multivariate statistics to identify features that correlate significantly with the $\delta^{13}\text{C}$ in respired CO₂ conditions, using orthogonal partial least squares-discriminant analysis (OPLS) with Simca[®], version 17.0.2 (Sartorius). In the OPLS, the response variable (Y variable) was $\delta^{13}\text{C}$ of respired CO₂ expressed relative to $\delta^{13}\text{C}$ in total organic matter (i.e., $\delta^{13}\text{C}_R - \delta^{13}\text{C}_{\text{OM}}$ denoted as $^{\text{OM}}\Delta\delta^{13}\text{C}_R$). We used $^{\text{OM}}\Delta\delta^{13}\text{C}_R$ to account for the fact that spinach and bean did not have the same range of $\delta^{13}\text{C}$ due to photosynthetic fixation. Also, for statistics, it was better to express $\delta^{13}\text{C}$ relative to organic matter rather than sugars (as in the model described below) to assess whether the $\Delta\delta^{13}\text{C}$ of sugars could be a driver of respired CO₂. The performance of the OPLS was assessed with the correlation between observed and predicted Y (R²), the cross validated correlation coefficient (Q²) and the P-value of the statistical model quantifying the probability that the OPLS model was not different from a random model mean±random error (this P-value is referred to as $P_{\text{CV-ANOVA}}$). Univariate analysis was also conducted via regression and calculation of the associated P-value. Volcano plots combine results from univariate (regression) and multivariate (OPLS) analyses, showing $-\log(P)$ versus OPLS loadings (illustrated in Figure 5).

2.11 | Nitrogen isotope mass balance

The proportion of ammonium in effective N utilisation (x) when ammonium and nitrate were present simultaneously was calculated by solving the mass-balance equation, as follows:

$$\delta^{15}\text{N}_{\text{obs}} = x \cdot (\delta^{15}\text{N}_a - \Delta_a) + (1-x) \cdot (\delta^{15}\text{N}_n - \Delta_n) \quad (1)$$

where subscript 'a' and 'n' refer to ammonium and nitrate respectively. Δ is the isotope fractionation during N assimilation (Δ_a and Δ_n were obtained under 100% ammonium and 100% nitrate, respectively), and $\delta^{15}\text{N}_{\text{obs}}$ is the weighted average of $\delta^{15}\text{N}$ of leaves and roots. Rearranging Equation 1 gives:

$$x = \frac{\delta^{15}\text{N}_{\text{obs}} - \delta^{15}\text{N}_n + \Delta_n}{\delta^{15}\text{N}_a - \Delta_a - \delta^{15}\text{N}_n + \Delta_n} \quad (2)$$

2.12 | Modelling

The $\delta^{13}\text{C}$ of night-time respired CO₂ was modelled using a metabolic mechanistic approach illustrated in Figure 6. It was assumed that the metabolically active pool of respiratory intermediates (organic acids) was fed by both stored organic acids (remobilisation, flux k_{-1}), glycolysis (s), and PEPC activity (p). This active pool is then used to produce CO₂ (respiration R), feed storage (flux k), and sustain amino acid synthesis and other metabolic pathways (utilisation u). Variation in pool size was assumed to be possible, i.e. the pool could be nonstationary. It was assumed that organic acids purified from organs

mostly reflected vacuolar material and thus their $\delta^{13}\text{C}$ were associated with stored organic acids. The change in pool size with time was denoted as a . Since the absolute $\delta^{13}\text{C}$ is dissimilar in spinach and bean due to different CO_2 source and photosynthetic isotope fractionation, $\delta^{13}\text{C}$ was expressed relative to source carbon, that is, the weighted average $\delta^{13}\text{C}$ of sugars (fructose, sucrose, glucose) (i.e., $\delta^{13}\text{C}_R - \delta^{13}\text{C}_{\text{sugars}}$ denoted as $\Delta\delta^{13}\text{C}_R$ in blue in Figure 6a).

The isoflux of ^{13}C in the active metabolic pool can be written as $\delta_{\text{act}} \cdot Q$, where δ_{act} is the isotope composition in the active pool and Q is the associated pool size. Therefore, the change in isoflux with time can be written as $d\delta_{\text{act}} \cdot Q/dt = Q \cdot d\delta_{\text{act}}/dt + \delta_{\text{act}} \cdot dQ/dt$, where the change in pool size with time is (by definition) dQ/dt and thus equals a . It should be noted that $d\delta_{\text{act}}/dt$ can be rewritten as $\delta_{\text{act}} \cdot d \ln(\delta_{\text{act}})/dt$. Therefore, $d\delta_{\text{act}} \cdot Q/dt$ can be written as $\delta_{\text{act}} \cdot (a + b)$ where $b = Q \cdot d \ln(\delta_{\text{act}})/dt$. In what follows, we will simplify notations and write $\delta_{\text{act}} \cdot a^*$ where $a^* = a + b$. The (differential) mass balance equation applied to δ_{act} is thus (neglecting second-order terms):

$$s \cdot (\delta_s - \Delta_s) + p \cdot \delta_{\text{fix}} + k_{-1} \cdot \delta_{\text{stock}} = R \cdot (\delta_{\text{act}} - \Delta_R) + u \cdot (\delta_{\text{act}} - \Delta_u) + k \cdot \delta_{\text{act}} + a^* \cdot \delta_{\text{act}} \quad (3)$$

Isotope fractionations are denoted as Δ . δ_s , δ_{stock} and δ_{fix} stand for the isotope composition in source sugars, stored organic acids, and carbon atom fixed by PEPC (from bicarbonate). Symbols and input values are summarised in Supporting Information S1: Table S1. In terms of carbon balance, we have: $s + p + k_{-1} = R + u + k + a^*$. This can be used to rearrange Equation 3 to:

$$\delta_{\text{act}} - \delta_s = \Delta\delta_{\text{act}} = \frac{R\Delta_R + u\Delta_u - s\Delta_s + p\Delta\delta_{\text{fix}} + k_{-1}\Delta\delta_{\text{stock}}}{R + k + a^* + u} \quad (4)$$

where isotope differences with source sugars are denoted as $\Delta\delta$. For simplicity, we assumed there was no isotope fractionation in glycolytic PEP production from sugars, therefore $\Delta_s = 0$. Thus, the associated term ($-s\Delta_s$) in the numerator of Equation 4 disappears. Note that Equation 4 assumes that storage and remobilisation of organic acids do not fractionate (transport between cellular compartments is unlikely to discriminate between isotopes to a great extent). Since the respiration rate varies between species and organs, it is more convenient to normalise with respiration R . Thus, we have:

$$\Delta\delta_{\text{act}} = \frac{\Delta_R + \frac{u}{R}\Delta_u + \frac{p}{R}\Delta\delta_{\text{fix}} + \frac{k_{-1}}{R}\Delta\delta_{\text{stock}}}{1 + \frac{k + a^*}{R} + \frac{u}{R}} \quad (5)$$

The isotope difference between sugars and respired CO_2 ($\Delta\delta^{13}\text{C}_R$) is then obtained from Equation 5 by subtracting the isotope fractionation associated with respiratory decarboxylations, Δ_R :

$$\Delta\delta^{13}\text{C}_R = \Delta\delta_{\text{act}} - \Delta_R \quad (6)$$

In Equation 5, p/R is known (since PEPC activity and respiration were measured) thus unknown relative metabolic fluxes are u/R , k_{-1}/R and $(k + a^*)/R$. These metabolic fluxes were not assumed to be

constant and rather, supposed to vary with $\text{NH}_4^+:\text{NO}_3^-$ nutrition, using a sigmoid (u/R , k_{-1}/R) or linear response ($k + a^*/R$; a linear response was chosen in this case since a^* contains a logarithm and thus an exponential component should transform to linear). $\Delta\delta_{\text{fix}}$ and $\Delta\delta_{\text{stock}}$ were known since they are the isotope difference between sugars and fixed bicarbonate, and between sugars and weighted average organic acids, respectively. $\Delta\delta_{\text{fix}}$ and $\Delta\delta_{\text{stock}}$ could thus be calculated for each sample. Solving (fitting) was performed using the Excel[®] solver, to optimise the match between predicted and observed $\Delta\delta^{13}\text{C}_R$ via the minimisation of the sum of squares. The value of embedded coefficients (particular, of sigmoid and linear responses) obtained by optimisation are listed in Supporting Information S1: Table S2.

3 | RESULTS

3.1 | N assimilation

The utilisation of nitrogen from source N of the nutrient solution was assessed using the nitrogen isotope composition ($\delta^{15}\text{N}$). The $\delta^{15}\text{N}$ of source ammonium, nitrate and total organic matter of leaves and roots is shown in Figure 1a. In both spinach and bean, leaves were slightly ^{15}N -enriched by 1‰–2‰ compared to roots. Spinach organic matter (in both leaves and roots) tended to be more ^{15}N -depleted than that of bean, suggesting that there was higher isotope fractionation during N assimilation in spinach. In fact, using 100% ammonium and 100% nitrate, the apparent isotope fractionation was calculated using the weighted average (biomass-weighted) of leaf and root $\delta^{15}\text{N}$. In bean, there was a fractionation in favour of ^{15}N by about 4‰ during ammonium utilisation (while there was almost no fractionation in spinach) and there was a small fractionation during nitrate utilisation, i.e., about 2‰ in spinach (against ^{15}N) and -0.5‰ (in favour of ^{15}N) in bean (Figure 1b, inset). Accounting for these isotope fractionations, we calculated the proportion of effective ammonium utilisation (Figure 1b). Effective ammonium utilisation closely followed the proportion of ammonium in source N, although it was slightly lower in bean than in spinach, suggesting that the two species were differentially selective for nitrate and ammonium. N conditions also influenced biomass and photosynthesis (summary of results in Supporting Information S1: Figures S1 and S2). As anticipated, ammonium caused a small decline in total plant biomass and at 100% ammonium, led to a significant drop in net photosynthesis. However, there was a concurrent change in stomatal conductance so that the intercellular-to-atmospheric CO_2 ratio (C_i/C_a) did not change dramatically.

3.2 | $\delta^{13}\text{C}$ of organic matter and respired CO_2

In both spinach (Figure 2a) and bean (Figure 2b), there was little change in $\delta^{13}\text{C}$ of total organic matter, suggesting that the photosynthetic isotope fractionation did not vary much. The

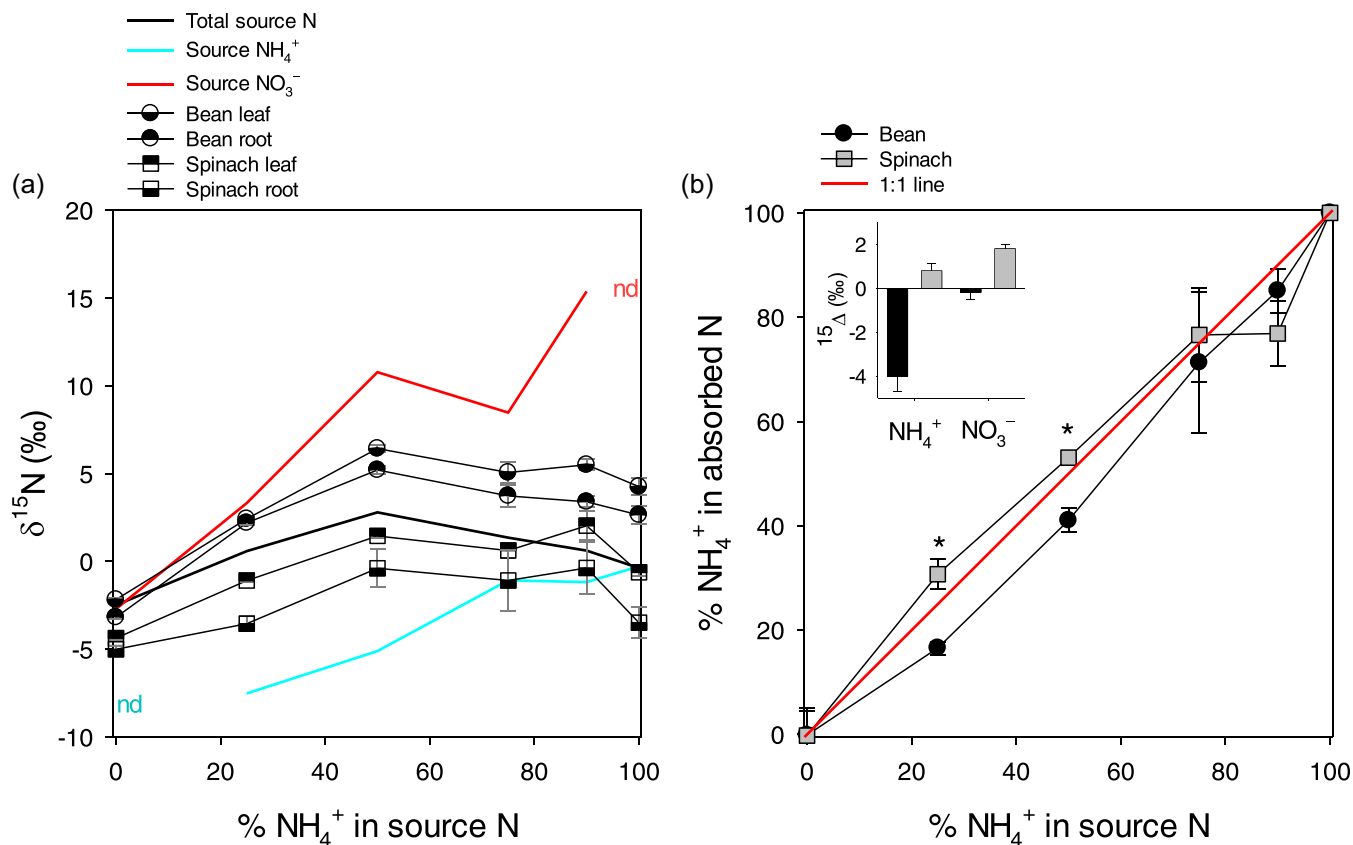


FIGURE 1 Nitrogen utilisation by plants: (a) nitrogen isotope composition in leaves and roots in bean (circles) and spinach (squares) compared to source total N (black line), where ammonium and nitrate moieties are shown in turquoise and red, respectively. (b) calculated proportion of effective ammonium utilisation in plants (in % of N used), with the 1:1 line in red. Inset, apparent $^{14}\text{N}/^{15}\text{N}$ isotope fractionation ($^{15}\Delta$, in per mil) during ammonium and nitrate utilisation in bean (black) and spinach (grey) (values obtained under pure ammonium and nitrate nutrition, respectively). A positive (resp. negative) value indicates a fractionation against ^{15}N (resp. ^{14}N). Asterisks stand for significant difference between species ($p < 0.05$). Values shown are means \pm SE ($n = 3$). The symbol 'nd' indicates situations where ammonium or nitrate $\delta^{15}\text{N}$ cannot be determined, simply because there is no ammonium (100% nitrate, red) and nitrate (100% ammonium, turquoise) in the solution, respectively.

comparison with maize organic matter cultivated under the same conditions (blue arrows in Figure 2) suggests that photosynthetic fractionation was slightly higher (about 21‰) in spinach than in bean (about 19‰). The $\delta^{13}\text{C}$ of water-soluble organic matter (WSOM) was relatively close to that in total organic matter and did not change considerably with $\text{NH}_4^+:\text{NO}_3^-$ nutrition. There was a relatively good agreement between the estimated isotope composition calculated with the photosynthetic isotope fractionation (Δ_i) and observed WSOM (Supporting Information S1: Figure S3). $\delta^{13}\text{C}$ of leaf-respired CO_2 decreased when the proportion of ammonium increased in source N (Figure 2a,c), with a depletion of about 4‰ in 100% ammonium compared to 100% nitrate. Such a decline was likely not due to a decline in photosynthetic isotope fractionation at least in spinach, since C_i/C_a decreased under high ammonium conditions, and thus photosynthetically fixed carbon was probably slightly ^{13}C -enriched (Supporting Information S1: Figures S2 and S3). The $\delta^{13}\text{C}$ of root-respired CO_2 did not change much, although it tended to be higher at 100% ammonium compared to 100% nitrate, by about 1‰ (Figure 2b,d).

3.3 | $\delta^{13}\text{C}$ of metabolites

The $\delta^{13}\text{C}$ varied considerably between metabolites (Figure 3), ranging between -40 and -25 ‰. There were considerable differences between sugar species, maltose being ^{13}C -enriched and glucose being ^{13}C -depleted. Malate was always relatively ^{13}C -enriched and was isotopically close to citrate (except in spinach leaves where it was about 2‰–3‰ ^{13}C -enriched compared to citrate). This suggests that malate carbon isotope composition was influenced by PEPC activity, which fixes ^{13}C -enriched bicarbonate to form C_4 acids. Amino acids tended to be ^{13}C -enriched with considerable variation. As expected for lipids, palmitate was generally ^{13}C -depleted, in particular compared to citrate and malate.

Taken as a whole, there was no consistent metabolic pattern of variation with respect to ammonium and nitrate proportions across organs and species. For example, amino acids were progressively ^{13}C -enriched as the proportion of ammonium increased in bean, but it was not the case in spinach. Interestingly, there were important changes in $\delta^{13}\text{C}$ of malate in spinach, with a maximum value

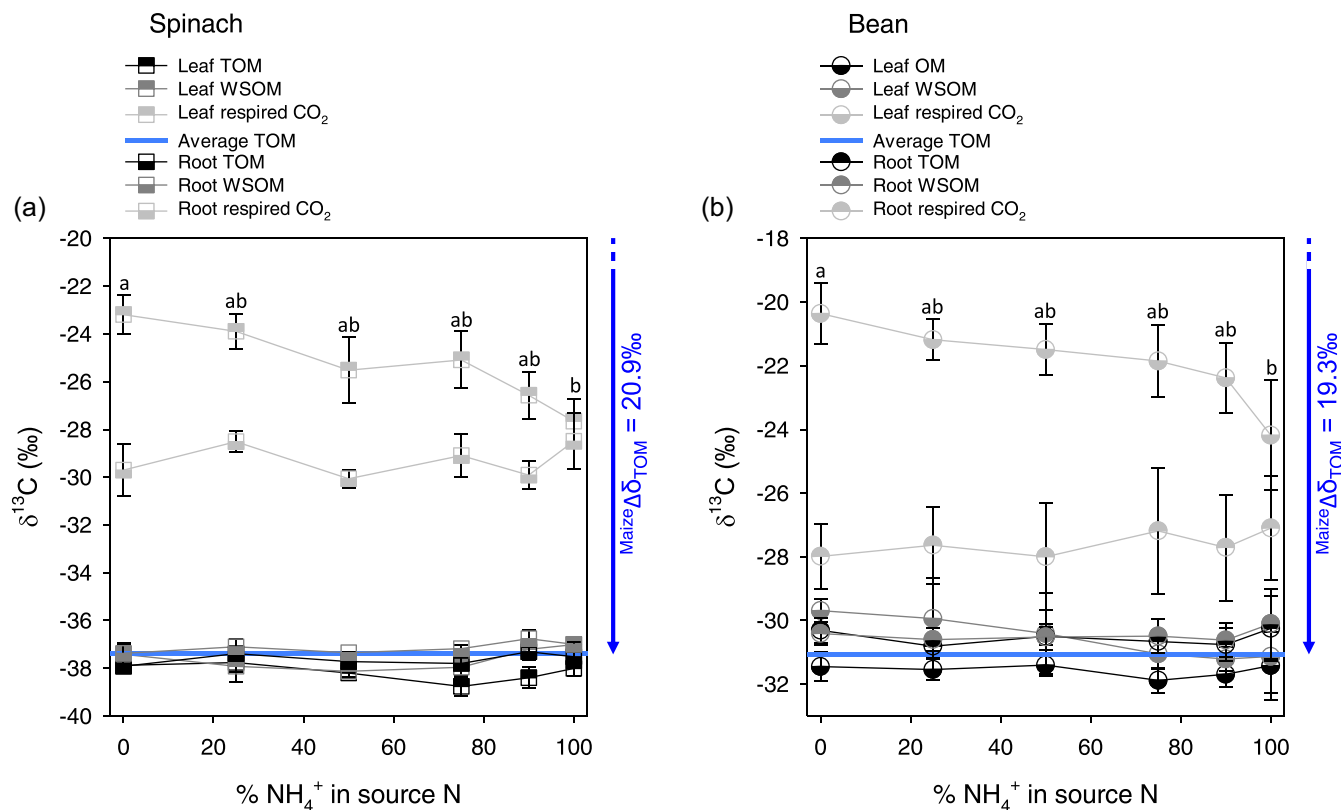


FIGURE 2 Carbon isotope composition in organic matter and respired CO_2 . The carbon isotope composition in total organic matter (black), water soluble fraction (dark grey) and respired CO_2 (light grey) are shown in spinach (a, squares) and bean (b, disks). blue horizontal lines stand for the average value of total organic matter (root and leaf) and the isotope difference with maize plants cultivated under the same conditions ($\text{Maize } \Delta\delta_{\text{TOM}}$) is shown with a blue arrow, providing a rough estimate of net photosynthetic isotope fractionation. Letters stand for statistical classes (one-way ANOVA, $p < 0.05$). Data shown are means \pm SE ($n = 3$). Scales are adjusted on y-axes to make the similarity of $\delta^{13}\text{C}$ variations in bean and spinach more visible.

(about -28‰) observed under 75% ammonium in leaves. Citrate tended to be enriched in ^{13}C by about 1‰ as ammonium proportion increased to 100%, except in spinach leaves where it reached a maximum at 75% ammonium, like malate. It is worth noting that except for maltose at high ammonium, no metabolite was more ^{13}C -enriched than respired CO_2 . It suggests that CO_2 generation by respiration was either (1) fed by a ^{13}C -enriched, small metabolic pool that was not well reflected by the isotope analysis of metabolites (i.e., total pools extracted from leaves and roots; Figure 3); or (2) associated with an isotope fractionation in favour of ^{13}C .

3.4 | Respiration, enzymatic activities and pool sizes

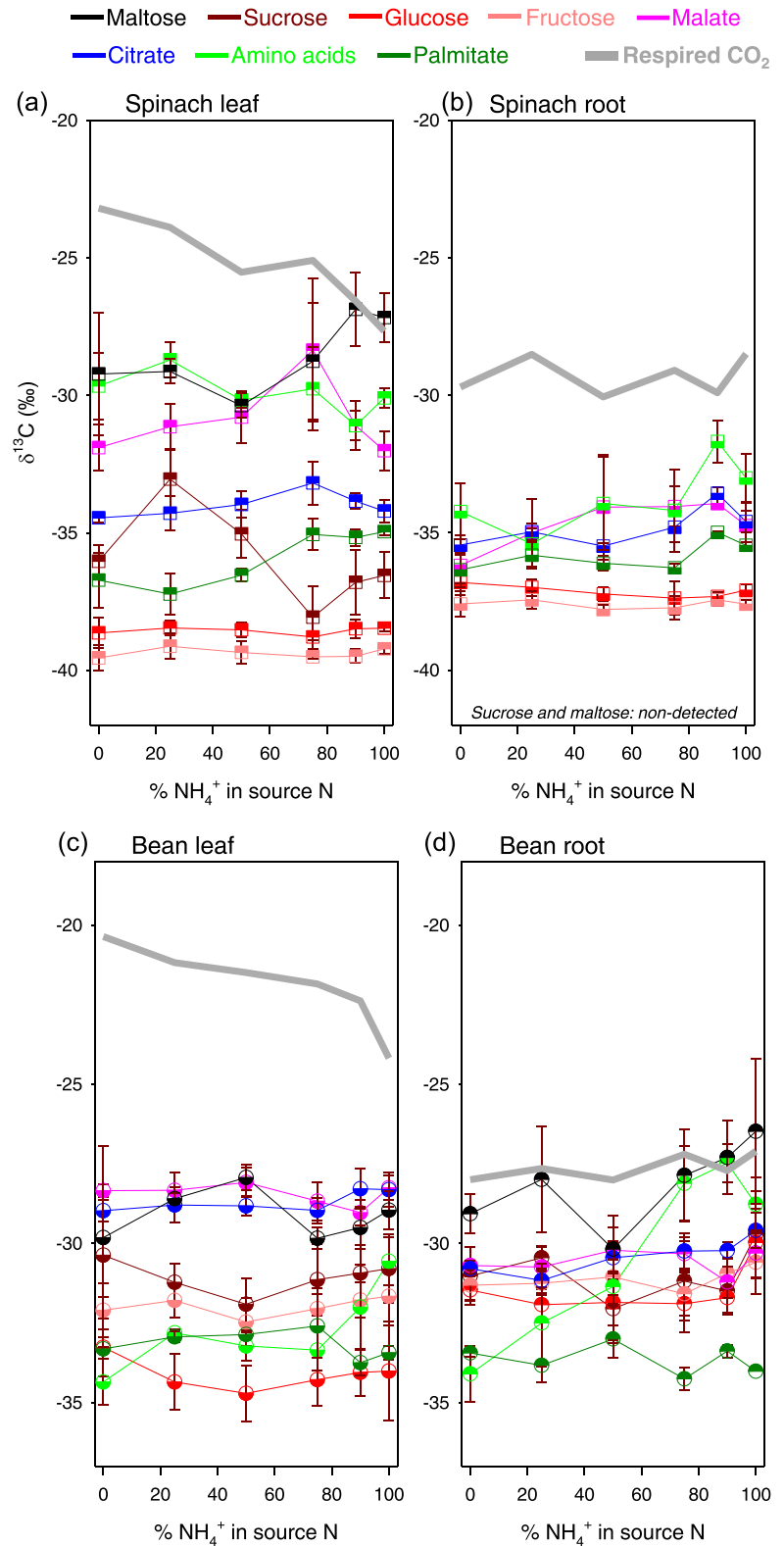
The respiration rate did not change considerably with $\text{NH}_4^+:\text{NO}_3^-$ ratio and was in the same order of magnitude ($20\text{--}40 \text{ nmol g}^{-1} \text{ s}^{-1}$) in bean organs and spinach leaves (Figure 4a). The respiration rate of spinach roots was comparatively high ($80\text{--}100 \text{ nmol g}^{-1} \text{ s}^{-1}$). PEPC activity tended to be higher in bean leaves when ammonium was less than 50% of source N but it was not affected by N nutrition in spinach leaves. PEPC activity in roots remained in the same order of

magnitude and was only significantly affected by N nutrition in bean roots with an increase under 100% ammonium (Figure 4b). Total sugar content was quite variable in leaves with no clear pattern when N nutrition changed (Figure 4c). Leaf malate decreased significantly as ammonium proportion increased; the citrate content decreased in bean leaves but was always very low in spinach leaves. A rather similar pattern in sugars, malate and citrate was observed in roots (Figure 4d), despite a progressive (insignificant) increase on average sugar content and an increase in spinach root malate content under 90% and 100% ammonium.

3.5 | Multivariate analysis of respired CO_2

We explored best drivers of $\delta^{13}\text{C}$ of respired CO_2 using a supervised multivariate method (OPLS), with $^{\text{OM}}\Delta\delta^{13}\text{C}_R$ as the response variable to be modelled. We used the full data set (i.e., all individual measurements, not average values) to assess whether it was possible to design a statistical model that was valid regardless of organs and species. Datapoints could be placed in the multivariate space according to $^{\text{OM}}\Delta\delta^{13}\text{C}_R$ along axis 1, with residual variance along axis 2 (Figure 5a). We obtained a very good statistical performance with R^2

FIGURE 3 Carbon isotope composition in leaf and root compounds. The $\delta^{13}\text{C}$ of major sugars, organic acids, amino acids and palmitate are shown with colours. The average $\delta^{13}\text{C}$ of respired CO_2 is traced with a thick grey line (values replotted from Figure 2). Here, $\delta^{13}\text{C}$ of amino acids is the weighted average of detected amino acids using GC-C-IRMS. The sugar labelled 'maltose' is used here as a generic term encapsulating either maltose or its β -stereoisomer cellobiose. Data shown are means \pm SE ($n = 3$). Note that in spinach roots, disaccharides were not detected and therefore sucrose and maltose are not shown. Scales are adjusted on y-axes to make the similarity of $\delta^{13}\text{C}$ variations in bean and spinach more visible.



of 0.81 (Figure 5b), high cross-validated coefficient Q^2 (0.77) and very high significance ($P_{\text{CV-ANOVA}} = 5.7 \cdot 10^{-19}$). Best drivers are shown as a volcano plot combining results of univariate and multivariate statistics (Figure 5c). The isotope composition in malate and citrate were the strongest drivers, followed by PEPC activity and various other

parameters. It demonstrates that respired CO_2 was determined by a combination of metabolic parameters (multivariate component) in which the isotope signature of organic acids had a relatively high weight. In other words, several metabolic fluxes and source metabolites are involved in the mechanism behind $\delta^{13}\text{C}$ of respired CO_2 .

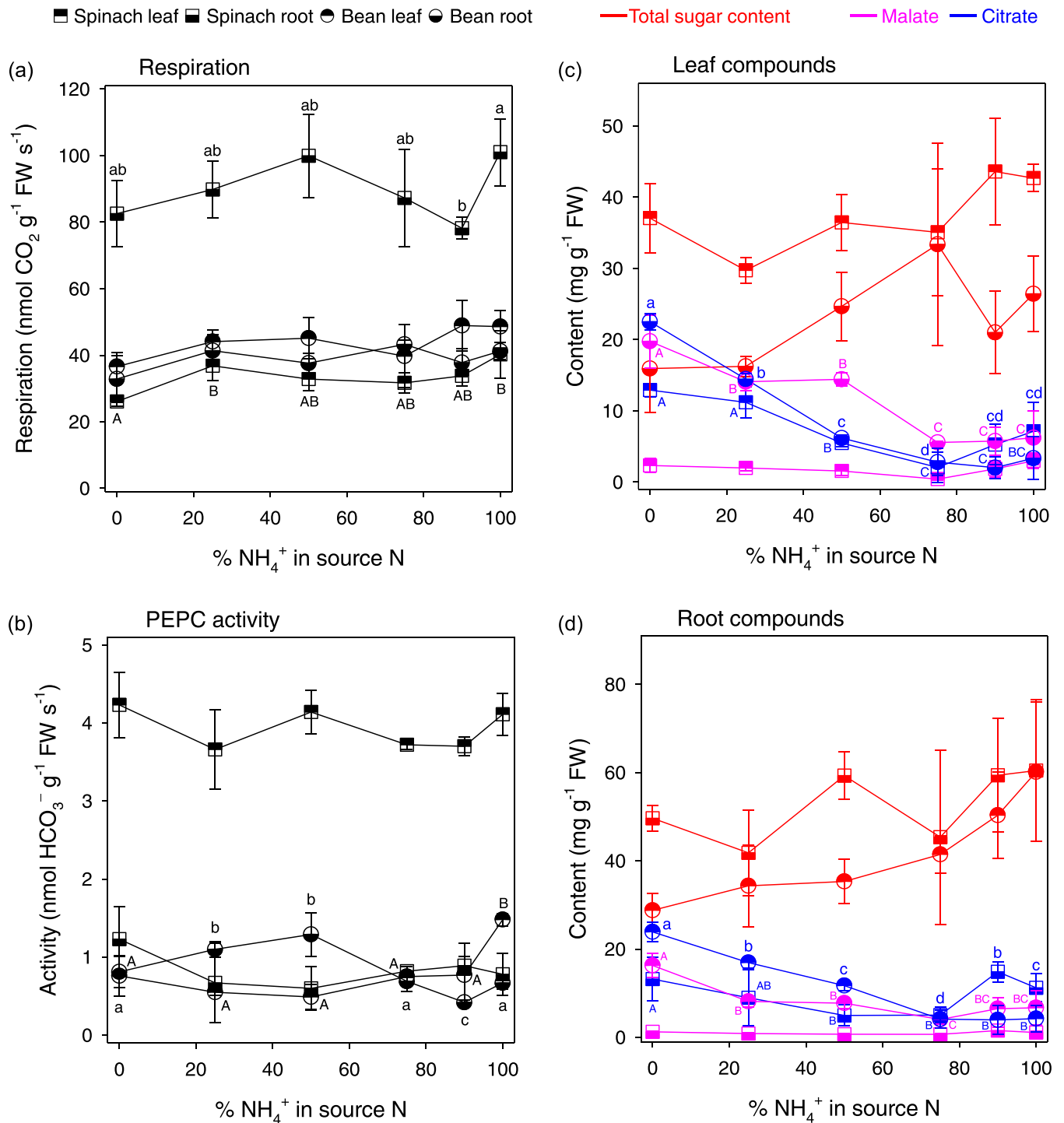


FIGURE 4 Metabolic properties: respiration (a), PEPC activity (b) per gram fresh weight (FW) and major compounds (c, d). In (c, d), the total sugar content represents the sum of sucrose, glucose and fructose. Letters stands for statistical classes when relevant (i.e. when significant differences are visible, $p < 0.05$).

3.6 | Modelling

A two-pool model was designed to compute the $\Delta\delta^{13}\text{C}_R$ as a function of source carbon, $\delta^{13}\text{C}$ of stored organic acids and metabolic fluxes (Figure 6a). Although simplistic, it should in principle capture the most important metabolic features that may

explain the isotope composition of respired CO_2 . Two flux parameters were known: respiration (R), PEPC activity (p). The glycolytic input (s) could be deduced from other parameters. Three input parameters, namely storage/build-up ($k + a^*$), remobilisation (k_{-1}) and utilisation (u) were unknown and their response function to ammonium was determined using least squares optimisation. Taken

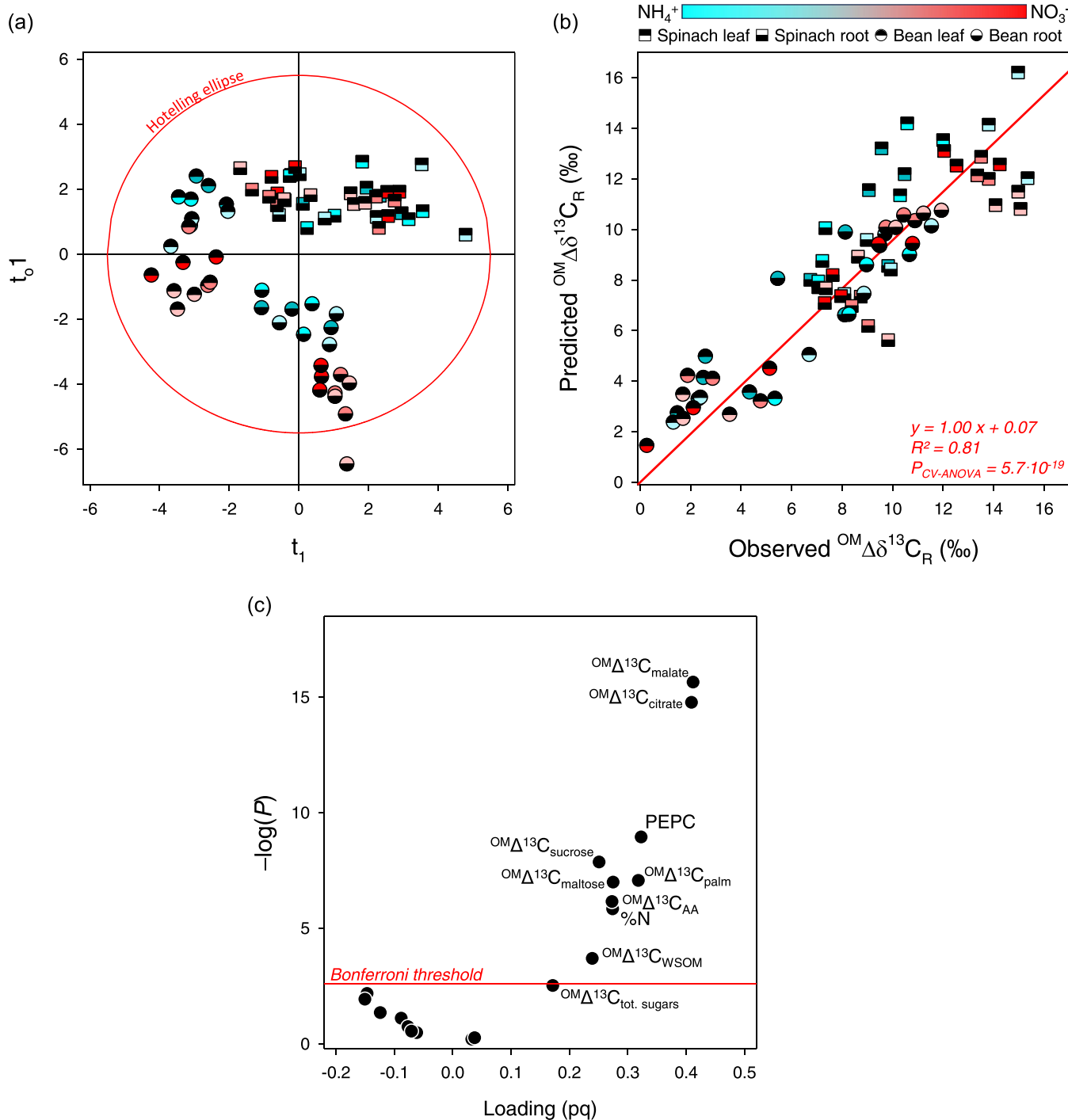


FIGURE 5 Statistical analysis of $\delta^{13}\text{C}$ of respired CO_2 . (a) Score plot of the supervised multivariate analysis (OPLS), with axis 1 (coordinate t_1) aligned with the response Y variable $\text{OM } \Delta^{13}\text{C}$ (isotope difference between organic matter and respired CO_2), and axis 2 (coordinate t_{01}) which is orthogonal to axis 1 (residual variance unrelated to that of $\delta^{13}\text{C}$ of respired CO_2). (b) Relationship between observed and OPLS-predicted $\text{OM } \Delta^{13}\text{C}$ (explaining 81% of variance). The linear regression is shown in red (symbols in legend). (c) Volcano plot showing the weight in the OPLS model (x axis) and the P -value (log₁₀ scale) of the regression (univariate analysis). The Bonferroni significance threshold (minimising the false discovery rate) is shown in red.

as a whole, the model explained quite well $\Delta\delta^{13}\text{C}$ (isotope difference between CO_2 and sugars) of respired CO_2 with a correlation coefficient (R^2) of 0.73 and a very close alignment to the 1:1 line (Figure 6b). Modelled storage, remobilisation and

utilisation increased with ammonium proportion while the glycolytic input decreased (Figure 6c). Interestingly, remobilisation and utilisation fluxes represented 1.5 to 4 times the respiration rate, showing that the respiratory metabolic pool was highly dynamic

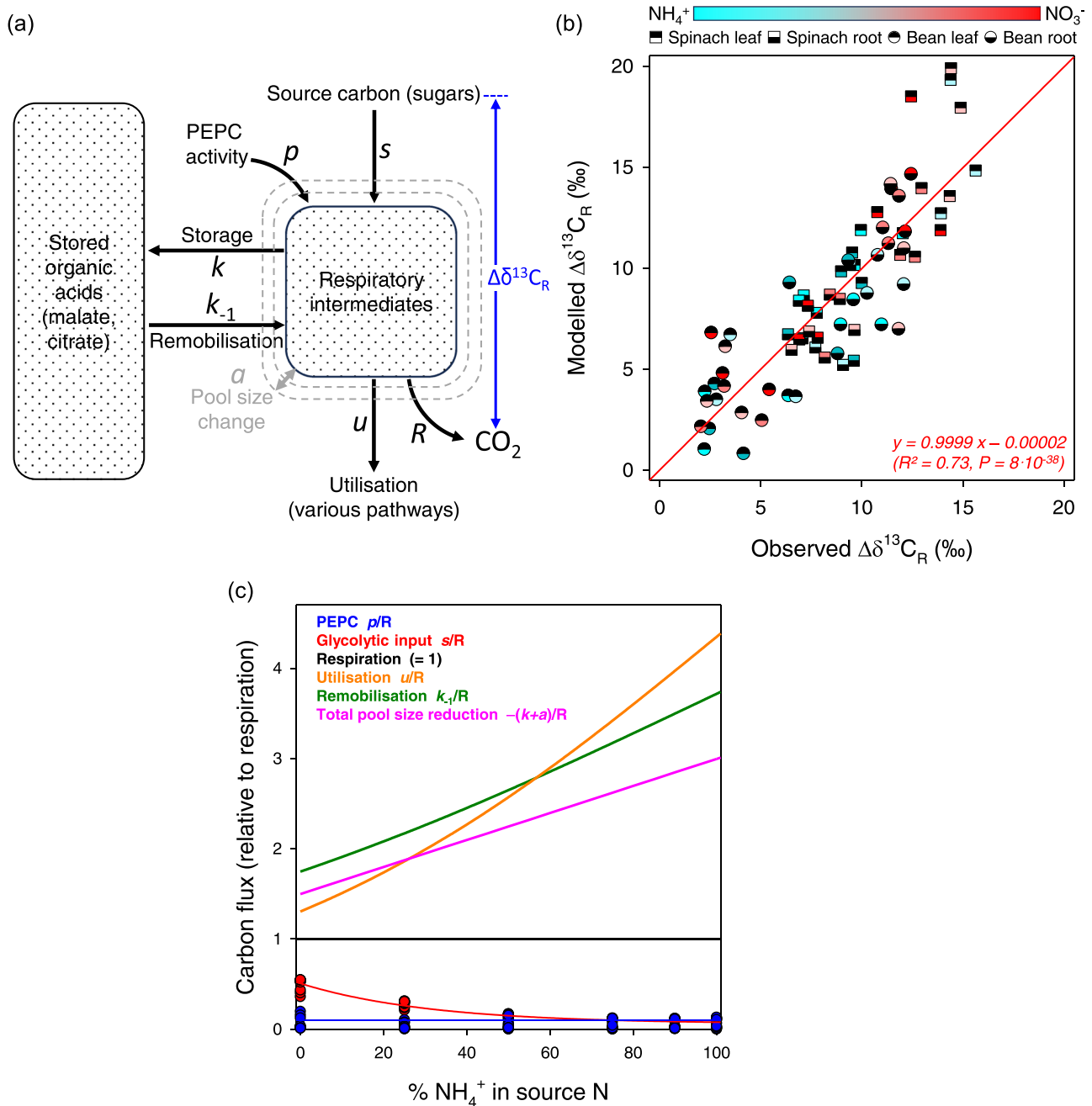


FIGURE 6 Calculation of the carbon isotope composition of respired CO_2 from metabolic data. (a) Two-box model used to calculate the isotopic difference between respired CO_2 and sugars ($\Delta\delta^{13}\text{C}_R$). See *Material and methods* for further modelling details. (b) Fit between modelled and observed $\Delta\delta^{13}\text{C}_R$ (symbols in legend). The red line stands for the regression (very close to the 1:1 line). The best fit (slope close to one and highest R^2) was obtained for a critical ammonium level of 100% used to describe the sigmoidal response of remobilisation (k_{-1}) and utilisation (u). (c) Values of model parameters as a function of ammonium availability. Note that PEPC activity (p) was not calculated since it was measured (= input parameter for each sample), and the glycolytic input (s) was calculated from other parameters for each sample. Fluxes are relative to respiration (thus respiration itself is constant and equal to 1, in black).

(high turn-over). Comparatively, the input of carbon by PEPC was small (a few percent of respiration) (see also Figure 4). There was also a predicted change in total pool size, with a more pronounced reduction in total organic acid pool as ammonium proportion increased (pink line, Figure 6c). It is worth noting that it is effectively what was observed with direct organic acid content measurements (Figure 4c,d).

4 | DISCUSSION

4.1 | Overall response of $\delta^{13}\text{C}$ in respired CO_2 to N nutrition

We found that unlike in roots, the carbon isotope composition of respired CO_2 in leaves decreased as the proportion of ammonium

increased in the N source (Figure 2). This pattern was remarkably similar in both species.

This effect was unlikely to be driven by N nutrition on photosynthetic isotope fractionation and thus on $\delta^{13}\text{C}$ of fixed carbon. First, no similar decrease in root-respired CO_2 was found (Figure 2), suggesting that metabolic, post-photosynthetic effects are involved. Second, variations (or the lack thereof) in C_i/C_a would lead to an increase (not a decrease) in $\delta^{13}\text{C}$ (Supporting Information S1: Figure S2). Similarly, (Høgh-Jensen & Schjoerring, 1997) reported that white clover plants supplied with nitrate had a lower apparent photosynthetic fractionation Δ than those supplied with ammonium. Conversely, Raven & Farquhar (1990) suggested that in nitrate-fed plants, there could be a lower C_i/C_a due to the combined effect of increased PEPC activity and higher photosynthetic capacity. Here, we found little change in $\delta^{13}\text{C}$ of total organic matter (Figure 2), also suggesting minimal effect of N conditions on photosynthetic fractionation. In results obtained so far, the impact of N nutrition on $\delta^{13}\text{C}$ of plant organic matter is variable, see for example (Brück & Guo, 2006; Guo et al., 2002) in bean. That said, we found here a slight ^{13}C -depletion in WSOM as the proportion of ammonium increased (Figure 2). This is also visible when WSOM is compared to predicted $\delta^{13}\text{C}$ of photosynthates (Supporting Information S1: Figure S3, points inside ellipses). It is more likely that under our conditions, WSOM was not properly representative of photosynthates, since the proportion of sugars and organic acids varied considerably (Figure 4) while their $\delta^{13}\text{C}$ differed considerably (Figure 3). In other words, WSOM was impacted by post-photosynthetic isotope fractionations in metabolism and its metabolic composition had an impact on its $\delta^{13}\text{C}$. In fact, when we calculated the weighted average of major compounds (organic acids and sugars), we could reconstruct the isotope signature of WSOM satisfactorily ($R^2 = 0.84$; Supporting Information S1: Figure S4).

We thus argue that the change in $\delta^{13}\text{C}$ of respired CO_2 as N nutrition varied was due to modifications in metabolism, leading to changes in respiratory substrates and/or in metabolic isotope fractionations. Accordingly, N nutrition had an influence on respiration, PEPC activity, sugar and organic acid content (Figure 4), the most visible effect being a decline in organic acids as the ammonium proportion increased. In bean, the sugar content changed little in leaves but increased significantly in roots under 100% NH_4^+ , while both malate and citrate contents decreased. This is consistent with previous reports (reviewed in Andrews et al., 2013; Britto & Kronzucker, 2013). It is believed that the biosynthesis of sugars and their storage in the vacuole under high NH_4^+ supply represent a detoxification strategy (Bittsánszky et al., 2015) while lower contents in malate and citrate reflect the disappearance of their metabolic function as nitrate proportion declines in the nutrient solution. In fact, under nitrate nutrition, a proportionally higher flux of PEPC activity is generally observed, allowing the formation of negative charges, counterbalancing excess inorganic cations and ensuring pH homeostasis (Krapp et al., 2014), as opposed to what occurs under ammonium nutrition (Britto & Kronzucker, 2002, 2005; Gerendás et al., 1997).

Surprisingly, there was no progressive decrease in PEPC activity as the ammonium proportion increased, under our conditions (except in bean leaves under high NH_4^+ , Figure 4b), despite the change in organic acid content. This demonstrates that N nutrition impacted various pathways and the relative flux of PEPC activity –rather than its absolute flux value– declined compared to other metabolic fluxes. This effect was visible in fitted relative flux values in Figure 6, where one can see that PEPC activity was always low under our conditions, while other flux values (such as utilisation and remobilisation) increased as ammonium proportion increased.

Interestingly, $\delta^{13}\text{C}$ of CO_2 respired by roots was not as ^{13}C -depleted as found previously (in practice, CO_2 was more ^{13}C -enriched than total root organic matter), for example in French bean (Bathellier et al., 2009). Therefore, under our experimental conditions, roots and leaves did not compensate for each other in terms of CO_2 loss, so that $\delta^{13}\text{C}$ of whole plant respired CO_2 was higher than, rather than equal to, $\delta^{13}\text{C}$ of whole plant organic matter (see *Introduction*). Such a situation has been encountered before in woody plants and occasionally in herbaceous species (reviewed in Ghashghaie & Badeck, 2014). Presumably, the isotope composition of root-respired CO_2 is very sensitive to metabolic differences between species and growth conditions. In addition, the sampling of root-respired CO_2 may involve root manipulation (e.g., washing, transfer in vials, etc.) and this could cause differences on average $\delta^{13}\text{C}$ between methods and laboratories. Effects of different methods for the preparation of roots for respiration measurements and diverse approaches for quantification of isofluxes should be scrutinised with further research.

4.2 | Is $\delta^{13}\text{C}$ of metabolites related to $\delta^{13}\text{C}$ of respired CO_2 ?

Variations in $\delta^{13}\text{C}$ of respired CO_2 was not simply caused by a source effect (i.e. change in respiratory substrate) and did not directly reflect changes in $\delta^{13}\text{C}$ of potential respiratory substrates (such as organic acids). In fact, we measured the carbon isotope composition of various metabolites (Figure 3) and found that (i) no specific metabolite had a response to N nutrition that was comparable to that of respired CO_2 ; and (ii) no metabolite was always as ^{13}C -enriched as respired CO_2 . In particular, we observed very limited changes in the $\delta^{13}\text{C}$ of soluble sugars (except for sucrose in spinach leaves) across N conditions. Interestingly, differences in carbon isotope composition between glucose, fructose and sucrose in leaves and roots were in line with previous findings: sucrose was considerably ^{13}C -enriched compared to glucose and fructose (Ghashghaie et al., 2001). We also note that maltose, which derives from starch degradation, was ^{13}C -enriched, in accordance with the general ^{13}C -enrichment in leaf starch compared to sucrose due to chloroplast enzymes isotope effects (Tcherkez et al., 2004). It is also unsurprising to observe some ^{13}C -enrichment in root sucrose (compared to glucose and fructose) too, since there is no isotope fractionation during sucrose export (Maunoury-Danger et al., 2009).

Organic acids were significantly ^{13}C -enriched relative to total soluble sugars, while the ^{13}C -difference between them was more pronounced in leaves than in roots. Unsurprisingly, malate exhibited a strong ^{13}C -enrichment, demonstrating the impact of the carbon input by PEPC activity. In fact, when dissolved CO_2 equilibrates with bicarbonate, the equilibrium isotope effect associated with bicarbonate formation enriches in ^{13}C by 9‰ (Marlier & O'Leary, 1984). Nevertheless, it should also be recognised that malate can be enriched as the result of isotope fractionations in malate degradation, leaving behind ^{13}C -enriched malate molecules. For example, the malic enzyme is associated with an isotope fractionation (kinetic isotope effect) of 32‰ for CO_2 liberation (C-4 atom of malate) (Edens et al., 1997). Parenthetically, it is remarkable that palmitate, which is synthesised from acetyl-CoA, shows limited changes in $\delta^{13}\text{C}$ overall (Figure 3, dark green), suggesting that metabolic modifications impacting $\delta^{13}\text{C}$ of respired CO_2 were downstream of pyruvate dehydrogenation (i.e., acetyl-CoA production), that is, in organic acid pool turn-over and/or Krebs cycle metabolism.

The $\delta^{13}\text{C}$ of amino acids showed a differential response in spinach and bean: while amino acids tended to be more ^{13}C -enriched as the ammonium proportion increased in bean, they remained stable in spinach (Figure 3, bright green). It suggests that the metabolism of amino acids incorporated ^{13}C -enriched material from carbon skeletons in bean, for example a greater proportion of ^{13}C -enriched respiratory substrates. In this species, the demand for carbon skeletons to assimilate N was probably higher since the elemental % of N was higher (Supporting Information S1: Figure S5). Also, bean appeared to be slightly more selective against ammonium under intermediate ammonium nutrition (Figure 1) and therefore high ammonium conditions can be expected to have a more drastic effect on amino acids.

4.3 | Metabolic origin of $\delta^{13}\text{C}$ of respired CO_2

Since potential respiratory substrates were not sufficiently enriched to account for the observed ^{13}C -enrichment in respired CO_2 , it was necessary to address metabolic determinants of CO_2 generation by respiration. The multivariate analysis conducted with all data points and samples suggested that CO_2 could be predicted statistically via a multivariate component comprising $\delta^{13}\text{C}$ of organic acids but also other variables including PEPC activity and $\delta^{13}\text{C}$ in other substrates (Figure 5c). Our results show the important role of the $\delta^{13}\text{C}$ in organic acids already found by Ghiasi et al. (2021) across $\text{NH}_4^+:\text{NO}_3^-$ ratios in tobacco leaves. Nevertheless, it should be noted that $\delta^{13}\text{C}$ of organic acids is always lower than that of respired CO_2 . As stated above, it indicates that there is either (a) a fractionation against ^{12}C during decarboxylations, or (b) utilisation of a ^{13}C -enriched pool that was not reflected in our compound-specific analysis (Figure 3). Hypothesis (a) is very unlikely since enzymes responsible for CO_2 production are associated with a normal kinetic isotope effect, i.e., against ^{13}C (Tcherkez et al., 2011). To our knowledge, there is only one

exception, namely NADP-dependent isocitrate dehydrogenase, which has a very small kinetic isotope effect (Grissom & Cleland, 1988) and may exhibit an inverse thermodynamic isotope effect at equilibrium (Lin et al., 2008). Hypothesis (b) is much more plausible, since the consumption of organic acids by catabolism, N assimilation, malic enzyme, conversion to C_5 branched acids, etc. likely fractionates against ^{13}C , leaving behind a ^{13}C -enriched pool (Rayleigh effect). In addition, this effect is believed to be responsible for the general ^{13}C -enrichment in $-\text{COOH}$ groups of organic acids (see, e.g., Hobbie & Werner, 2004; Schmidt, 2003), along with the natural ^{13}C -enrichment in C-atom positions C-3 and C-4 of glucose, that are at the origin of C-atoms (COOH group) decarboxylated by pyruvate dehydrogenase (Gilbert et al., 2012; Rossmann et al., 1991).

We explored the credibility of hypothesis (b) with a model that accounts for the co-occurrence of a metabolically active pool and a pool of stored organic acids (described by Equations 4 and 5 in *Material and methods*). In fact, the model could generate relative $\delta^{13}\text{C}$ of respired CO_2 ($\Delta\delta^{13}\text{C}_R$) in broad agreement with observed values ($R^2 = 0.73$; Figure 6b). Interestingly, such an agreement was observed regardless of species and organs, suggesting that the metabolic mechanism explaining the $\delta^{13}\text{C}$ of respired CO_2 was sufficiently generic. We recognise that there is still substantial variance (27%), due to probable species and organ effects as well as the contribution of metabolic pathways not accounted for, like OPPP. Modelling confirmed (1) the critical influence of the turn-over of the metabolically active pool, fed by remobilisation and used by respiration and other uses (with flux value that were relatively high); and (2) the fact that non-stationarity is probably important. In practice, it means that during plant development or during a diel cycle, the metabolically active organic acid pool is very dynamic and thus when respired CO_2 is sampled, this pool is probably not in the steady state. Such a non-stationarity contributes to the observed ^{13}C -enrichment because organic acids are consumed by fractionating reactions, thereby exaggerating the ^{13}C -enrichment in acids left behind. Our results further suggest that this effect depends on N conditions, simply because utilisation, remobilisation and variation in pool size are impacted by the $\text{NH}_4^+:\text{NO}_3^-$ balance (Figure 6c).

4.4 | Perspectives

Taken as a whole, our results show that $\delta^{13}\text{C}$ of respired CO_2 is not simply linked to a unique metabolic source but rather, is a combination of flux values and $\delta^{13}\text{C}$ of different components and this could be made apparent via both multivariate and modelling approaches. We nevertheless recognise that the drivers of respired CO_2 found here may not apply to other situations, such as prolonged darkness (where the shift from sugar consumption to lipid degradation is involved) or the transition from light to dark in leaves (where light-enhanced dark respiration relates to malate degradation by the malic enzyme). Still, in all cases, emphasis should be given to non-stationarity of metabolic pools and substrates used by respiration. That is, respiratory substrates are very dynamic and

their modification or their turn-over contributes to the observed ^{13}C -signature of respired CO_2 . Of course, we also recognise that our modelling exercise was very simplified, since it did not account for all metabolic fluxes and furthermore, disregarded intramolecular isotope compositions. As stated above, there are important $\delta^{13}\text{C}$ differences between C-atom positions, including those in organic acids. Unfortunately, there is presently no method implementable routinely to analyse $\delta^{13}\text{C}$ of organic acids. Typically, using quantitative ^{13}C -NMR would require sample preparation to convert COOH groups to their reduced forms ($-\text{CH}_2\text{OH}$), break molecular symmetry (e.g., in the case of citrate) and block configuration changes and equilibria. To our knowledge, no such method has been published yet. This technical challenge will be addressed in a subsequent study so as to gain further insights into the isotope signature of CO_2 generated by plant respiration.

ACKNOWLEDGEMENTS

Yang Xia wishes to thank the China Scholarship Council (CSC) for her PhD scholarship funding. The authors are grateful to Laboratoire d'Ecologie, Systématique et Evolution, ESE (University of Paris-Sud, Orsay, France) for the financial support of the experiments; Laboratory of ECOSYS (INRA, Grignon) for training on and assistance in isotope analyses of respired CO_2 ; Annika Ackermann and Institute of Agricultural Sciences (ETH Zürich) for isotope analyses of organic material; Steffen Ruelow and Max Planck Institute (Jena, Germany) for training on and assistance in LC-C-IRMS analyses of sugars and organic acids; Marlène Lamothe-Sibold for training on EA-IRMS; and the gardeners of ESE for helping in plant culture/care. Guillaume Tcherkez thanks the financial support by the Région Pays de la Loire and Angers Loire Métropole via the grant Connect Talent Iseseed.

CONFLICT OF INTEREST STATEMENT

The authors declare no conflict of interest.

DATA AVAILABILITY STATEMENT

All data are shown in main text or supplementary material.

ORCID

Yang Xia  <http://orcid.org/0000-0001-9842-030X>

Franz-W. Badeck  <http://orcid.org/0000-0001-7821-8825>

Cyril Girardin  <http://orcid.org/0000-0002-4684-1222>

Camille Bathellier  <http://orcid.org/0000-0003-4952-4713>

Gerd Gleixner  <http://orcid.org/0000-0002-4616-0953>

Roland A. Werner  <http://orcid.org/0000-0002-4117-1346>

Guillaume Tcherkez  <http://orcid.org/0000-0002-3339-956X>

Jaleh Ghashghaie  <http://orcid.org/0000-0002-2381-8396>

REFERENCES

- A. Hobbie, E. & Werner, R.A. (2004) Intramolecular, compound-specific, and bulk carbon isotope patterns in C_3 and C_4 plants: a review and synthesis. *New Phytologist*, 161(2), 371–385.
- Andrews, M. (1986) The partitioning of nitrate assimilation between root and shoot of higher plants. *Plant, Cell & Environment*, 9(7), 511–519.
- Andrews, M., Raven, J.A. & Lea, P.J. (2013) Do plants need nitrate? The mechanisms by which nitrogen form affects plants. *Annals of Applied Biology*, 163(2), 174–199.
- Barbour, M.M., McDowell, N.G., Tcherkez, G., Bickford, C.P. & Hanson, D.T. (2007) A new measurement technique reveals rapid post-illumination changes in the carbon isotope composition of leaf-respired CO_2 . *Plant, Cell & Environment*, 30(4), 469–482.
- Barbour, M.M., Ryazanova, S. & Tcherkez, G. (2017) Respiratory effects on the carbon isotope discrimination near the compensation point. In: Tcherkez, G. & Ghashghaie, J. (Eds.) *Plant respiration: Metabolic fluxes and carbon balance*, 43. Springer, pp. 143–160.
- Bathellier, C., Badeck, F.W., Couzi, P., Harscoët, S., Mauve, C. & Ghashghaie, J. (2008) Divergence in $\delta^{13}\text{C}$ of dark respired CO_2 and bulk organic matter occurs during the transition between heterotrophy and autotrophy in *Phaseolus vulgaris* plants. *New Phytologist*, 177(2), 406–418.
- Bathellier, C., Badeck, F.-W. & Ghashghaie, J. (2017) Carbon Isotope Fractionation in Plant Respiration. In: Tcherkez, G. & Ghashghaie, J. (Eds.) *Plant respiration: Metabolic fluxes and carbon balance*. Springer, pp. 43–68.
- Bathellier, C., Tcherkez, G., Bligny, R., Gout, E., Cornic, G. & Ghashghaie, J. (2009) Metabolic origin of the $\delta^{13}\text{C}$ of respired CO_2 in roots of *Phaseolus vulgaris*. *New Phytologist*, 181(2), 387–399.
- Bittsánszky, A., Pilinszky, K., Gyulai, G. & Komives, T. (2015) Overcoming ammonium toxicity. *Plant Science*, 231, 184–190.
- Britto, D.T. & Kronzucker, H.J. (2002) NH_4^+ toxicity in higher plants: a critical review. *Journal of Plant Physiology*, 159(6), 567–584.
- Britto, D.T. & Kronzucker, H.J. (2005) Nitrogen acquisition, PEP carboxylase, and cellular pH homeostasis: new views on old paradigms. *Plant, Cell & Environment*, 28(11), 1396–1409.
- Britto, D.T. & Kronzucker, H.J. (2013) Ecological significance and complexity of N-source preference in plants. *Annals of Botany*, 112(6), 957–963.
- Brück, H. & Guo, S. (2006) Influence of N form on growth photosynthesis of *Phaseolus vulgaris* L. plants. *Journal of Plant Nutrition and Soil Science*, 169(6), 849–856.
- Domergue, J.B., Abadie, C., Lalande, J., Deswarte, J.C., Ober, E., Laurent, V. et al. (2022) Grain carbon isotope composition is a marker for allocation and harvest index in wheat. *Plant, Cell & Environment*, 45(7), 2145–2157.
- Domergue, J.-B., Lalande, J., Abadie, C. & Tcherkez, G. (2022) Compound-specific $^{14}\text{N}/^{15}\text{N}$ analysis of amino acid trimethylsilylated derivatives from plant seed proteins. *International Journal of Molecular Sciences*, 23(9), 4893.
- Edens, W.A., Urbauer, J.L. & Cleland, W.W. (1997) Determination of the chemical mechanism of malic enzyme by isotope effects. *Biochemistry*, 36(5), 1141–1147.
- Gerendás, J., Zhu, Z., Bendixen, R., Ratcliffe, R.G. & Sattelmacher, B. (1997) Physiological and biochemical processes related to ammonium toxicity in higher plants. *Zeitschrift für Pflanzenernährung und Bodenkunde*, 160(2), 239–251.
- Gessler, A., Tcherkez, G., Karyanto, O., Keitel, C., Ferrio, J.P., Ghashghaie, J. et al. (2009) On the metabolic origin of the carbon isotope composition of CO_2 evolved from darkened light-acclimated leaves in *Ricinus communis*. *New Phytologist*, 181(2), 374–386.
- Ghashghaie, J. & Badeck, F.W. (2014) Opposite carbon isotope discrimination during dark respiration in leaves versus roots—a review. *New Phytologist*, 201(3), 751–769.
- Ghashghaie, J., Duranceau, M., Badeck, F.W., Cornic, G., Adeline, M.T. & Deleens, E. (2001) $\delta^{13}\text{C}$ of CO_2 respired in the dark in relation to $\delta^{13}\text{C}$ of leaf metabolites: comparison between *Nicotiana sylvestris* and *Helianthus annuus* under drought. *Plant, Cell & Environment*, 24(5), 505–515.

- Ghiasi, S., Lehmann, M.M., Badeck, F.W., Ghashghaie, J., Hänsch, R., Meinen, R. et al. (2021) Nitrate and ammonium differ in their impact on $\delta^{13}\text{C}$ of plant metabolites and respired CO_2 from tobacco leaves. *Isotopes in Environmental and Health Studies*, 57(1), 11–34.
- Gilbert, A., Robins, R.J., Remaud, G.S. & Tcherkez, G.G.B. (2012) Intramolecular ^{13}C pattern in hexoses from autotrophic and heterotrophic C_3 plant tissues. *Proceedings of the National Academy of Sciences*, 109(44), 18204–18209.
- González-Moro, M.B., González-Moro, I., De la Peña, M., Estavillo, J.M., Aparicio-Tejo, P.M., Marino, D. et al. (2021) A multi-species analysis defines anaplerotic enzymes and amides as metabolic markers for ammonium nutrition. *Frontiers in Plant Science*, 11, 632285.
- Grissom, C.B. & Cleland, W.W. (1988) Isotope effect studies of the chemical mechanism of pig heart NADP isocitrate dehydrogenase. *Biochemistry*, 27(8), 2934–2943.
- Guo, S., Brück, H. & Sattelmacher, B. (2002) Effects of supplied nitrogen form on growth and water uptake of French bean (*Phaseolus vulgaris* L.) plants. *Plant and Soil*, 239(2), 267–275.
- Høgh-Jensen, H. & Schjoerring, J. (1997) Effects of drought and inorganic N form on nitrogen fixation and carbon isotope discrimination in *Trifolium repens*. *Plant Physiology and Biochemistry*, 35, 55–62.
- Klumpp, K., Schäufele, R., Lötscher, M., Lattanzi, F.A., Feneis, W. & Schnyder, H. (2005) C-isotope composition of CO_2 respired by shoots and roots: fractionation during dark respiration? *Plant, Cell & Environment*, 28(2), 241–250.
- Knohl, A., Werner, R.A., Brand, W.A. & Buchmann, N. (2005) Short-term variations in $\delta^{13}\text{C}$ of ecosystem respiration reveals link between assimilation and respiration in a deciduous forest. *Oecologia*, 142(1), 70–82.
- Krapp, A., David, L.C., Chardin, C., Girin, T., Marmagne, A., Leprince, A.-S. et al. (2014) Nitrate transport and signalling in arabidopsis. *Journal of Experimental Botany*, 65(3), 789–798.
- Lehmann, M.M., Wegener, F., Barthel, M., Maurino, V.G., Siegwolf, R.T.W., Buchmann, N. et al. (2016) Metabolic fate of the carboxyl groups of malate and pyruvate and their influence on $\delta^{13}\text{C}$ of leaf-respired CO_2 during light enhanced dark respiration. *Frontiers in Plant Science*, 7, 190574.
- Lin, Y., Volkman, J., Nicholas, K.M., Yamamoto, T., Eguchi, T., Nimmo, S.L. et al. (2008) Chemical mechanism of homoisocitrate dehydrogenase from *Saccharomyces cerevisiae*. *Biochemistry*, 47(13), 4169–4180.
- Marlier, J.F. & O'Leary, M.H. (1984) Carbon kinetic isotope effects on the hydration of carbon dioxide and the dehydration of bicarbonate ion. *Journal of the American Chemical Society*, 106(18), 5054–5057.
- Maunoury-Danger, F., Bathellier, C., Laurette, J., Fresneau, C., Ghashghaie, J., Damesin, C. et al. (2009) Is there any $^{12}\text{C}/^{13}\text{C}$ fractionation during starch remobilisation and sucrose export in potato tubers? *Rapid Communications in Mass Spectrometry*, 23(16), 2527–2533.
- Priault, P., Wegener, F. & Werner, C. (2009) Pronounced differences in diurnal variation of carbon isotope composition of leaf respired CO_2 among functional groups. *New Phytologist*, 181(2), 400–412.
- Raven, J.A. & Farquhar, G.D. (1990) The influence of N metabolism and organic acid synthesis on the natural abundance of isotopes of carbon in plants. *New Phytologist*, 116(3), 505–529.
- Rossmann, A., Butzenlechner, M. & Schmidt, H.-L. (1991) Evidence for a nonstatistical carbon isotope distribution in natural glucose. *Plant Physiology*, 96(2), 609–614.
- Schmidt, H.-L. (2003) Fundamentals and systematics of the non-statistical distributions of isotopes in natural compounds. *Naturwissenschaften*, 90, 537–552.
- Stitt, M. (2002) Steps towards an integrated view of nitrogen metabolism. *Journal of Experimental Botany*, 53(370), 959–970.
- Tcherkez, G., Farquhar, G., Badeck, F. & Ghashghaie, J. (2004) Theoretical considerations about carbon isotope distribution in glucose of C_3 plants. *Functional Plant Biology*, 31(9), 857–877.
- Tcherkez, G., Mahé, A. & Hodges, M. (2011) $^{12}\text{C}/^{13}\text{C}$ fractionations in plant primary metabolism. *Trends in Plant Science*, 16(9), 499–506.
- Tcherkez, G., Nogués, S., Bleton, J., Cornic, G., Badeck, F. & Ghashghaie, J. (2003) Metabolic origin of carbon isotope composition of leaf dark-respired CO_2 in French bean. *Plant Physiology*, 131(1), 237–244.
- Werner, C. & Gessler, A. (2011) Diel variations in the carbon isotope composition of respired CO_2 and associated carbon sources: a review of dynamics and mechanisms. *Biogeosciences*, 8(9), 2437–2459.
- Werner, C., Unger, S., Pereira, J.S., Ghashghaie, J. & Máguas, C. (2007) Temporal dynamics in $\delta^{13}\text{C}$ of ecosystem respiration in response to environmental changes. *Terrestrial Ecology*, 1, 191–210.
- Werner, R.A., Bruch, B.A. & Brand, W.A. (1999) ConFlo III—an interface for high precision $\delta^{13}\text{C}$ and $\delta^{15}\text{N}$ analysis with an extended dynamic range. *Rapid Communications in Mass Spectrometry*, 13(13), 1237–1241.
- Xiao, C., Fang, Y., Wang, S. & He, K. (2023) The alleviation of ammonium toxicity in plants. *Journal of integrative plant biology*, 65(6), 1362–1368.

SUPPORTING INFORMATION

Additional supporting information can be found online in the Supporting Information section at the end of this article.

How to cite this article: Xia, Y., Lalande, J., Badeck, F.-W., Girardin, C., Bathellier, C., Gleixner, G. et al. (2024) Nitrogen nutrition effects on $\delta^{13}\text{C}$ of plant respired CO_2 are mostly caused by concurrent changes in organic acid utilisation and remobilisation. *Plant, Cell & Environment*, 47, 5511–5526. <https://doi.org/10.1111/pce.15062>